Bioorganic & Medicinal Chemistry xxx (2012) xxx–xxx

Contents lists available at SciVerse ScienceDirect

Bioorganic & Medicinal Chemistry

journal homepage: www.elsevier.com/locate/bmc

Inhibitors of Dengue virus and West Nile virus proteases based on the aminobenzamide scaffold

Sridhar Aravapalli [a], Huiguo Lai [b], Tadahisa Teramoto [b], Kevin R. Alliston [a], Gerald H. Lushington [c], Eron L. Ferguson [a], R. Padmanabhan [b], William C. Groutas [a,*]

[a] Department of Chemistry, Wichita State University, Wichita, KS 67260, USA
[b] Department of Microbiology and Immunology, Georgetown University Medical Center, Washington, DC 20057, USA
[c] Molecular Graphics and Modeling Laboratory, The University of Kansas, Lawrence, KS 66045, USA

ARTICLE INFO

Article history:
Received 23 February 2012
Revised 19 April 2012
Accepted 27 April 2012
Available online xxxx

Keywords:
Protease
Dengue virus
West Nile virus
Aminobenzamide

ABSTRACT

Dengue and West Nile viruses (WNV) are mosquito-borne members of flaviviruses that cause significant morbidity and mortality. There is no approved vaccine or antiviral drugs for human use to date. In this study, a series of functionalized *meta* and *para* aminobenzamide derivatives were synthesized and subsequently screened in vitro against Dengue virus and West Nile virus proteases. Four active compounds were identified which showed comparable activity toward the two proteases and shared in common a *meta* or *para*(phenoxy)phenyl group. The inhibition constants (K_i) for the most potent compound **7n** against Dengue and West Nile virus proteases were 8.77 and 5.55 μM, respectively. The kinetics data support a competitive mode of inhibition of both proteases by compound **7n**. This conclusion is further supported by molecular modeling. This study reveals a new chemical scaffold which is amenable to further optimization to yield potent inhibitors of the viral proteases via the combined utilization of iterative medicinal chemistry/structure–activity relationship studies and in vitro screening.

1. Introduction

The Dengue virus (DENV) and West Nile Virus (WNV) are members of the family *Flaviviridae* which comprise several human and animal pathogens, including Yellow fever virus (YFV), Hepatitis C virus (HCV), and Japanese encephalitis virus (JEV).[1] Infection by DENV1–4 serotypes results in Dengue fever which can progress to life-threatening Dengue hemorrhagic fever (DHF) and Dengue shock syndrome (DSS).[2] Dengue infection is a global health threat for which there are currently no small molecule antiviral therapeutics or effective vaccines. Inhibition of DENV replication constitutes a promising avenue of investigation for the development of therapeutics against DENV.[3–5]

Both Dengue and West Nile viruses are small, enveloped viruses containing a positive-stranded 11-kb RNA genome which encodes a polyprotein precursor which is co- and post-translationally processed by host cell proteases and the viral encoded trypsin-like protease, NS2B/NS3, into three structural proteins (C, prM, E) and seven non-structural proteins (NS1, NS2A, NS2B, NS3, NS4A, NS4B, and NS5).[6,7] NS3 is a multi-functional protein containing a serine protease with a prototypical catalytic triad (H51, D75, S135) within the N-terminal 185 amino acid residues, an NTPase/RNA helicase, and a 5′-RNA triphosphatase within the C-terminal (161–618 amino acid residues) region of NS3.[4–6] Activation of the serine protease domain of NS3 requires NS2B cofactor, a ~130 amino acid hydrophobic integral membrane protein in the endoplasmic reticulum (ER). A ~45 amino acid conserved hydrophilic segment from the NS2B sequence is sufficient for interaction with and activation of the NS3 protease domain for protease activity (hereafter referred to as 'NS2B/NS3pro') in vitro.[5,7,8] Processing of the polyprotein by NS2B/NS3pro is essential for viral replication, consequently NS2B/NS3pro has emerged as an attractive target for the discovery and development of small molecule therapeutics for DENV infection.[3–6]

DENV NS2B/NS3pro has a substrate specificity for an –X–K–R–R–G/S– sequence corresponding to the subsites $-S_4-S_3-S_2-S_1-S'_1-$.[9] Cleavage is at the $P_1-P'_1$ (R–G/S) scissile bond. The hydrophilic β-hairpin segment of the NS2B protein cofactor wraps around the NS3 protease core and is required for optimal catalytic efficiency.[10–12] Crystallographic[12,13] and high-field NMR studies[14] have illuminated greatly our understanding of the role played by the NS2B cofactor and the nature of the interaction of NS2B/NS3pro with small-molecule inhibitors.

DENV NS2B/NS3pro plays a vital role in virus replication, consequently, orally-bioavailable drug-like agents that inhibit NS2B/NS3pro are of value as potential therapeutics for DENV infection. Inhibitors of NS2B/NS3pro containing a highly charged peptidyl recognition element with a dibasic motif at P_1-P_2 coupled to an

* Corresponding author. Tel.: +1 316 978 7374; fax: +1 316 978 3431.
E-mail address: bill.groutas@wichita.edu (W.C. Groutas).

0968-0896/$ - see front matter © 2012 Elsevier Ltd. All rights reserved.
http://dx.doi.org/10.1016/j.bmc.2012.04.055

array of electrophilic warheads (aldehydes, trifluoromethyl ketones, and boronic acids),[15–18] non-peptidyl α-ketoamides,[19] phthalazine-based derivatives,[20] arylcyanoacrylamides,[21] retro peptide-hybrids,[22] benz[*d*]isothiazol-3(2*H*)-one derivatives,[23] and others[24] have been reported. We describe herein the results of synthetic and biochemical studies related to the inhibition of DENV and WNV NS2B/NS3pro by functionalized *para*- and *meta*-substituted aminobenzamide derivatives represented by structure (I) (Fig 1).

2. Chemistry

Compounds **7a–t** (Table 1) and **8a–f** (Table 2) were synthesized starting with methyl *p*-aminobenzoate or methyl *m*-aminobenzoate, respectively, as illustrated in Scheme 1. Thus, treatment with trichloromethyl chloroformate yielded the corresponding isocyanate which was reacted with propargylamine to form urea derivatives **2a–b**. Click chemistry[25] with an array of structurally diverse azides yielded the corresponding functionalized urea derivatives which were further elaborated to form the final compounds.

3. Biochemistry

The expression and purification of DENV NS2B/NS3pro and WNV NS2B/NS3pro have been previously described.[26–28] Enzyme assays and inhibition studies were carried out as previously described[29–31] and the results are summarized in Fig. 2–4 and Tables 3 and 4.

4. Results and discussion

The world-wide health problem stemming from infection by Dengue virus and related flaviviruses, as well as the paucity of small-molecule therapeutics for combating flavivirus infection, have provided the impetus for the research described herein. The aminobenzamide scaffold was utilized in the synthesis of a series of structurally-diverse *meta* and *para*-substituted derivatives, represented by general structure (I), (Fig 1). The design of (I) rested on the following considerations: (a) the shallow active site of DENV NS2B/NS3pro presents a formidable challenge in terms of the design of potent inhibitors of the enzyme, necessitating the use of a suitably-embellished multifunctional molecule capable of engaging in multiple favorable binding interactions with the enzyme in order to attain high potency, without compromising oral bioavailability and PK characteristics.[32–39] The problem is further compounded by the stringent substrate specificity requirements of the protease for positively charged substrates/inhibitors; (b) based on insights gained from examining the X-ray crystal structures of DENV2 NS2B/NS3pro with bound ligands[12,13] and molecular modeling studies, it was hypothesized that the utilization of a planar platform capable of orienting appended non-peptidyl recognition elements in a precisely-defined vector relationship would lead to agents capable of interacting with multiple active site residues. Thus, the aminobenzamide platform was chosen for generating the desired compounds and for conducting exploratory studies. An added advantage is the flexibility afforded by the two points of diversity in the chosen scaffold, augmenting synthetic tractability; (c) a urea functionality was initially employed to lessen the conformational flexibility of the appended recognition elements. The latter included an electron-rich heterocycle having multiple hydrogen bond acceptor sites linked to an aryl–alkyl group and, (d) it was furthermore envisaged that the initial attachment of an array of structurally-diverse aliphatic and aromatic amines to the carboxyl group of the aminobenzamide scaffold would provide additional binding sites.

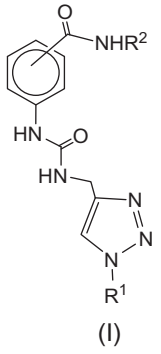

(I)

Figure 1. General structure of aminobenzamide derivatives (I).

The desired compounds were readily obtained as shown in Scheme 1. These were subsequently screened against DENV NS2B/NS3pro and WNV NS2B/NS3pro. Four of the compounds based on (I) were found to exhibit activity against both proteases and the results are summarized in Table 3 and Fig 2. It can be generally inferred from the SAR studies that the nature of both R_1 and R_2 influence activity. Furthermore, activity is manifested when R_1 is a *meta* or *p*-(phenoxy)phenyl group. All other amides were inactive, suggesting that the *meta* or *p*-(phenoxy)phenyl group is accommodated in a hydrophobic cleft. It should be noted that some of the compounds were inactive despite the presence of a *meta* or *p*-(phenoxy)phenyl group (compounds **7a** and **8f**).

The percent inhibition shown by compound **7n** against both DENV2 and WNV was found to be higher than any of the other selected compounds (Fig 2). The apparent IC_{50} values of compound **7n** (Fig 3) were determined to be 6.82 ± 0.09 and 5.51 ± 0.08 μM against DENV2 and WNV protease, respectively. We also performed kinetics analyses to determine the K_m, k_{cat} and V_{max} values in the presence and absence of compound **7n** at four different concentrations (Fig 4 and Table 4). The apparent Michaelis–Menten constants ($K_{m,app}$) increased and k_{cat}/K_m decreased proportionally with increasing concentration of compound **7n**. The results support a competitive mode of inhibition. Next, we employed molecular modeling to identify a plausible binding mode for **7n**. Based on the molecular docking simulations, a high affinity bound conformer that is similar in both the DENV and WNV proteases was identified. Docking poses analysis yielded only one high potency conformer (i.e., one of the top five scoring poses) that conserved most of the key interactions in both DENV and WNV (Fig. 5A and 5B, respectively). Key features of this pose that are conserved across the two receptors include π–π stacking interactions between the ligand fluorobenzyl group and the side chain of Tyr161, and hydrophobic interactions between the ligand phenoxyphenyl group and Val72. Visual inspection suggests that these interactions are not only conserved but are also likely to comprise most of the favorable binding features in both cases. Furthermore confidence in this proposed pharmacophore is attained through comparison with predicted binding modes for inactive compounds **7a** and **8f**. In the case of DENV NS2B/NS3pro in Fig 5A, neither of the inactive compounds is predicted to exploit either of the two lipophiles listed above with the same effectiveness as **7n**: compound **8f** has poor overlap with both lipophiles, and while compound **7a** is predicted to achieve some π–π stacking with Tyr161, its furan group is not situated anywhere near any lipophiles. In the case of WNV NS2B/NS3pro (Fig 5B), reasonable π–π stacking is achieved with Tyr161 in all cases, but the furan group of **7a** is again poorly situated, while the phenoxyphenyl group of **8f** is not predicted to derive nearly as much a hydrophobic interaction as is achieved by the corresponding phenoxyphenyl group of **7n**, whose terminal phenyl group is predicted to wedge favorably between Val72 and the lipophilic portion of neighboring Lys73.

Table 1
p-Aminobenzamide compounds

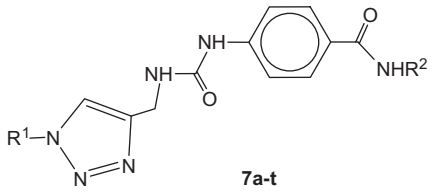

7a-t

Compound	R^1	R^2	Compound	R^1	R^2
7a	Phenylthiomethyl	4-Phenoxyphenyl	**7k**	Benzyl	2-Furanylmethyl
7b	Phenylthiomethyl	Benzyl	**7l**	Benzyl	2-Morpholinoethyl
7c	Phenylthiomethyl	Phenylethyl	**7m**	Benzyl	3-Phenoxyphenyl
7d	Phenylthiomethyl	Phenyl	**7n**	4-Fluorobenzyl	4-Phenoxyphenyl
7e	Phenylthiomethyl	2-Furanylmethyl	**7o**	4-Fluorobenzyl	Benzyl
7f	Phenylthiomethyl	2-Morpholinoethyl	**7p**	4-Fluorobenzyl	Phenylethyl
7g	Benzyl	4-Phenoxyphenyl	**7q**	4-Fluorobenzyl	Phenyl
7h	Benzyl	Benzyl	**7r**	4-Fluorobenzyl	2-Furanylmethyl
7i	Benzyl	Phenylethyl	**7s**	4-Fluorobenzyl	2-Morpholinomethyl
7j	Benzyl	Phenyl	**7t**	4-Fluorobenzyl	3-Phenoxyphenyl

Table 2
m-Aminobenzamide compounds

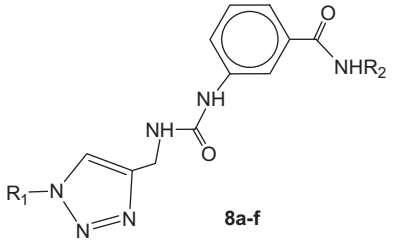

8a-f

Compound	R^1	R^2
8a	Phenylthiomethyl	Benzyl
8b	Phenylthiomethyl	Phenylethyl
8c	Phenylthiomethyl	3-Phenoxyphenyl
8d	Benzyl	Benzyl
8e	Benzyl	Phenylethyl
8f	Benzyl	3-Phenoxyphenyl

In summary, the studies described herein have demonstrated that the aminobenzamide scaffold can be employed in the synthesis of inhibitors of DENV and WNV NS2B/NS3pro.

5. Experimental section

5.1. General

The ^{1}H spectra were recorded on a Varian XL-300 or XL-400 NMR spectrometer. Melting points were determined on a Mel-Temp apparatus and are uncorrected. High resolution mass spectra (HRMS) were performed at the University of Kansas Mass Spectrometry Lab. Reagents and solvents were purchased from various chemical suppliers (Aldrich, Acros Organics, TCI America, and Bachem). Silica gel (230–450 mesh) used for flash chromatography was purchased from Sorbent Technologies (Atlanta, GA). Thin layer chromatography was performed using Analtech silica gel plates. The TLC plates for the final compounds were eluted using two different solvent systems and were visualized using iodine and/or UV light. Each individual compound was identified as a single spot on TLC plate (purity was greater than 95% by ^{1}H NMR). DENV2 NS2B/NS3 pro (or WNV NS2B/NS3 pro) substrate Bz-Nle-Lys-Arg-Arg-AMC was purchased from Bachem, Torrance, CA or custom synthesized by NeoBioScience, Cambridge, MA.

5.2. Representative syntheses

5.2.1. Compound 1a

To methyl 4-aminobenzoate (30.23 g; 200 mmol) in anhydrous 1,4-dioxane (500 mL) was added trichloromethyl chloroformate (59.35 g; 300 mmol) dropwise and the reaction mixture was refluxed for 8 h. The solvent was removed on the rotary evaporator to yield **1a** as a yellow solid, which was purified by vacuum distillation to give a yellow solid (34 g, 96% yield). IR (neat) ν_{NCO} 2268 cm^{-1}. ^{1}H NMR ($CDCl_3$): δ 3.88 (s, 3H), 7.14–7.18 (m, 2H), 7.96–8.02 (m, 2H).

5.2.2. Compound 1b

Brown solid (94% yield). IR (neat) ν_{NCO} 2257 cm^{-1}. ^{1}H NMR ($CDCl_3$): δ 3.93 (s, 3H), 7.28–7.29 (m, 1H), 7.37–7.44 (m, 1H), 7.76–7.78 (1H), 7.85–7.89 (m, 1H).

5.2.3. Compound 2a

To a solution of **1a** (15.06 g; 85 mmol) in anhydrous THF (150 mL) was added propargylamine (4.68 g; 85 mmol). The reaction mixture was stirred at room temperature overnight. The precipitate formed was collected by suction filtration to give **2a** as a white solid (18.5 g; 94% yield), mp 175–177 °C. ^{1}H NMR (DMSO-d_6): δ 3.13 (t, J = 2.45 Hz, 1H), 3.80 (s, 3H), 3.88 (dd, J = 5.70, 2.48 Hz, 2H), 6.71 (t, J = 5.69 Hz, 1H), 7.46–7.59 (m, 2H), 7.78–7.91 (m, 2H), 9.11 (s, 1H).

5.2.4. Compound 2b

White solid (90% yield), mp 158–160 °C. ^{1}H NMR (DMSO-d_6): δ 3.11 (t, J = 2.46 Hz, 1H), 3.84 (s, 3H), 3.88 (dd, J = 5.72, 2.46 Hz, 2H), 6.61 (t, J = 5.73 Hz, 1H), 7.37 (t, J = 7.87 Hz, 1H), 7.49–7.52 (m, 1H), 7.58–7.62 (m, 1H), 8.12 (t, J = 1.80 Hz, 1H), 8.94 (s, 1H).

5.2.5. Compound 3a

Compound **2a** (11.61 g; 50 mmol) and phenylthiomethyl azide (8.26 g; 50 mmol) were suspended in a 1:1 mixture of *t*-butanol and water (100 mL). Sodium ascorbate (1.00 g; 5 mmol) and $CuSO_4{\cdot}5H_2O$ (0.12 g; 0.5 mmol) were then added and the heterogeneous mixture was stirred vigorously at room temperature for 2 days. The progress of the reaction was monitored by TLC. The reaction mixture was diluted with water (200 mL) and cooled in an ice bath. The precipitate formed was collected by suction filtration to give **3a** as an off-white powder (19.47 g, 98% yield), mp 155–157 °C. ^{1}H NMR ($CDCl_3$): δ 3.88 (s, 3H), 4.48 (d,

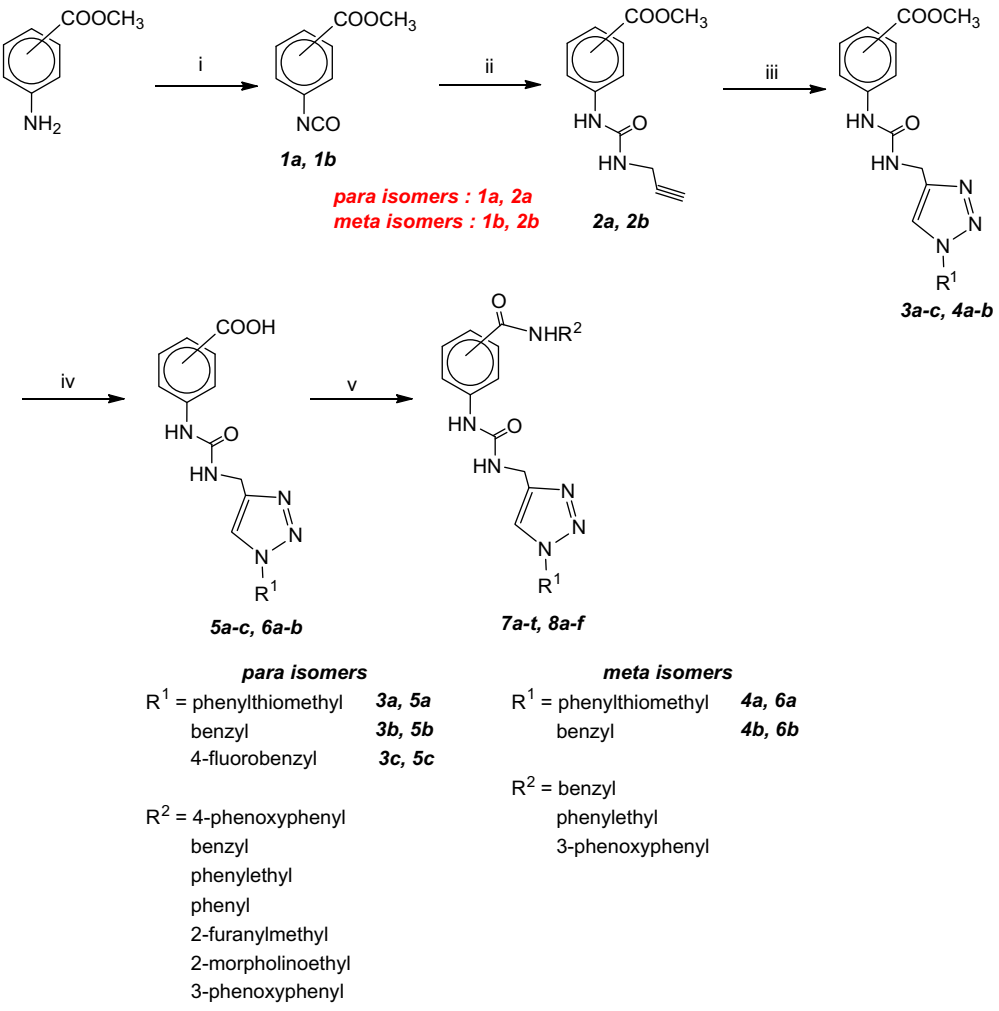

Scheme 1. Reagents and conditions: (i) Trichloromethyl chloroformate/THF, Δ; (ii) propargl amine/THF; (iii) arklalkyl azide *t*-BuOH and H_2O sodium ascorbate; (iv) aqLiOH/1,4-dioxane; (V) CD/THF, followed by amine.

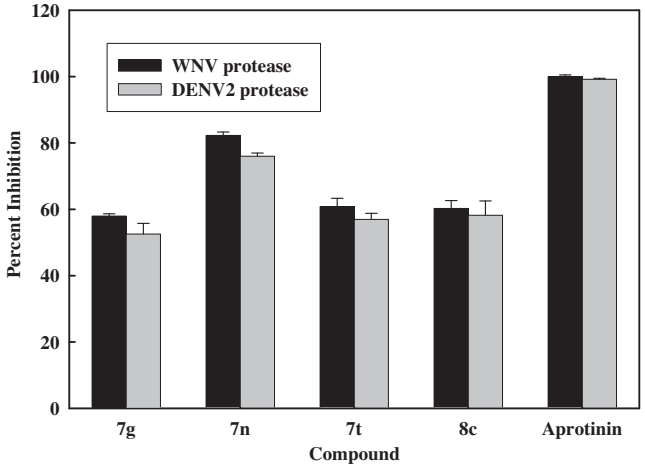

Figure 2. Inhibition of DENV2 and WNV NS2B/NS3pro by selected compounds at 25 μM. The concentrations of WNV and DENV2 NS2B/NS3pro protease were 28 and 25 nM, respectively. The buffer used contained 200 mM Tris–HCl, 6.0 mM NaCl, 30% glycerol, and 0.1% CHAPS, pH 9.5. The percent values were calculated from the relative fluorescence units obtained in the presence and absence of tested compound. BPTI (Aprotinin) and DMSO were used as a positive and negative control, respectively. All assays were performed in triplicate and the average values are shown.

J = 5.84 Hz, 2H), 5.58 (s, 2H), 6.86 (t, *J* = 4.92 Hz, 1H), 7.21–7.34 (m, 5H), 7.39–7.42 (m, 2H), 7.66 (s, 1H), 7.91 (d, *J* = 8.73 Hz, 3H).

5.2.6. Compound 3b

Light green solid (93% yield), mp 175–177 °C. ^{1}H NMR (DMSO-d_6): δ 3.79 (s, 3H), 4.34 (d, *J* = 5.51 Hz, 2H), 5.57 (s, 2H), 6.79 (br s, 1H), 7.28–7.40 (m, 5H), 7.50–7.53 (m, 2H), 7.82–7.84 (m, 2H), 8.02 (s, 1H), 9.03 (s, 1H).

5.2.7. Compound 3c

Light green solid (100% yield), mp 194–195 °C. ^{1}H NMR (DMSO-d_6): δ 3.79 (s, 3H), 4.33 (d, *J* = 5.55 Hz, 2H), 5.56 (s, 2H), 6.78 (t, *J* = 5.61, Hz, 1H), 7.17–7.23 (m, 2H), 7.36–7.41 (m, 2H), 7.50–7.54 (m, 2H), 7.82–7.84 (m, 2H), 8.03 (s, 1H), 9.03 (s, 1H).

5.2.8. Compound 4a

White solid (80% yield). ^{1}H NMR (DMSO-d_6): δ 3.83 (s, 3H), 4.29 (d, *J* = 5.67 Hz, 2H), 5.92 (s, 2H), 6.69 (t, *J* = 5.67 Hz, 1H), 7.25–7.42 (m, 6H), 7.48–7.51 (m, 1H), 7.56–7.59 (m,1H), 7.91 (s, 1H), 8.13 (t, *J* = 1.92 Hz, 1H), 8.89 (s, 1H).

5.2.9. Compound 4b

White solid (66% yield), mp 158–160 °C. ^{1}H NMR (DMSO-d_6): δ 3.83 (s, 3H), 4.33 (d, *J* = 5.47 Hz, 2H), 5.57 (s, 2H), 6.66 (t,

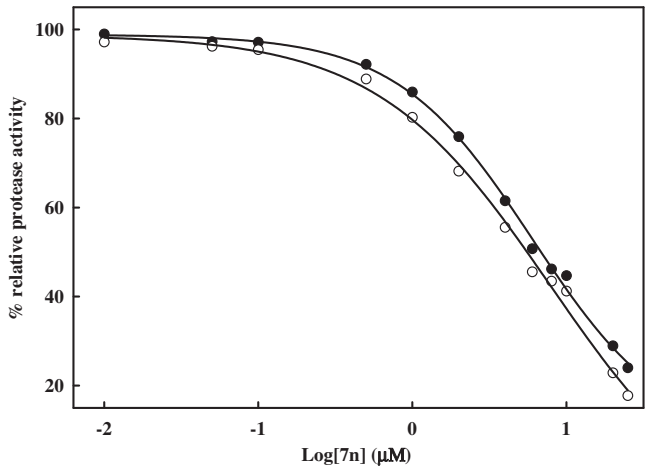

Figure 3. Determination of IC_{50} value of the inhibitor **7n** against DENV-2 and WNV protease. The inhibitor was incubated with DENV2 NS2B/NS3pro (25 nM) or WNV NS2B/NS3pro (28 nM) in buffer (200 mM Tris–HCl, 6 mM NaCl and 30% glycerol, pH 9.5) for 15 min. Bz-Nle-Lys-Arg-Arg-AMC (5.0 μM) was added to the mixture in a final volume of 100 μL. The fluorescence intensity was measured at 460 nm with excitation at 380 nm and converted to the percentage of protease activity in the absence and presence of inhibitors. The solid line is the theoretical fitting curve based on the Sigmoidal equation.[40] The apparent IC_{50} values for compound **7n** were 6.82 ± 0.09 and 5.51 ± 0.08 μM against DENV-2 (solid circle) and WNV (open circle), respectively.

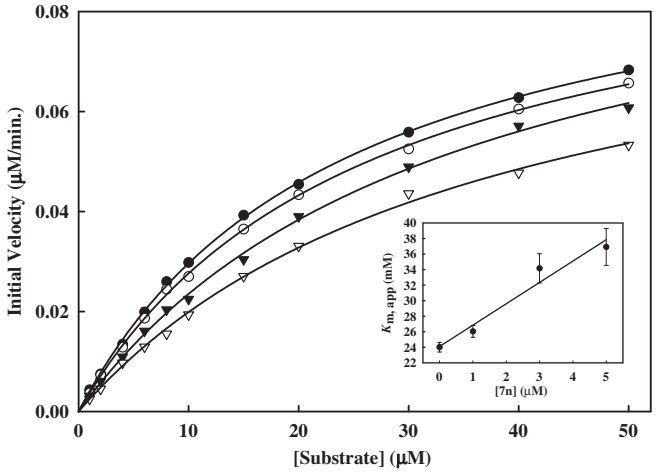

Figure 4. Inhibition of WNV NS2B/NS3pro protease activity by compound **7n**. Initial reaction rates of the substrate (Bz-Nle-Lys-Arg-Arg-AMC) cleavage catalyzed by WNV NS2B/NS3pro protease (28 nM) in 200 mM Tris–HCl (pH 9.5), 6.0 mM NaCl, 30% glycerol and 0.1% CHAPS at 37 °C were determined by varying the substrate concentrations in the range of 0, 1, 2, 4, 6, 8, 10, 15, 20, 30, 40 and 50 μM at each concentration of inhibitor fixed at 0 (solid circle), 1.0 μM (open circle), 3.0 μM (solid triangle) and 5.0 μM (open triangle). The reactions were initiated by the addition of WNV NS2B/NS3pro protease and the fluorescence intensity at 460 nm was monitored with an excitation at 380 nm. Reactions were less than 5% completion in all cases to maintain valid steady-state measurements. The solid lines are fitted lines using the Michaelis–Menten equation. Inset: Secondary plot of $K_{m,app}$ against the concentration of compound **7n**. Kinetics studies were carried out as described utilizing substrate concentrations of 0–50 μM Bz-Nle-Lys-Arg-Arg-AMC. Each experiment was performed in duplicate and repeated three times. Data were analyzed using SigmaPlot 2001 v7.0 software[40] to determine values for apparent K_m and k_{cat}.

J = 5.37 Hz, 1H), 7.29–7.40 (m, 6H), 7.48–7.50 (m, 1H), 7.56–7.59 (m, 1H), 8.02 (s, 1H), 8.13 (t, J = 1.76 Hz, 1H), 8.84 (s, 1H)

5.2.10. Compound 5a

To a solution of ester **3a** (17 g; 42.5 mmol) in 1,4-dioxane (500 mL) was added a solution of LiOH (12.21 g; 510 mmol) in water (150 mL) and the reaction mixture was stirred at room temperature overnight. The reaction mixture was cooled in an ice bath and a 5% HCl solution was added dropwise until the pH was ~3. The precipitate formed was collected by suction filtration to give acid **5a** as a white solid (18.64 g, 97% yield), mp >230 °C. ^{1}H NMR (DMSO-d_6): δ 4.30 (d, J = 5.61 Hz, 2H), 5.93 (s, 2H), 6.77 (t, J = 5.67 Hz, 1H), 7.23–7.42 (m, 5H), 7.48–7.51 (m, 2H), 7.80–7.83 (m, 2H), 7.92 (s, 1H), 9.01 (s, 1H), 12.49–12.72 (br s, 1H).

5.2.11. Compound 5b

White solid (87% yield), mp >230 °C. ^{1}H NMR (DMSO-d_6): δ 4.33 (s, 2H), 5.57 (s, 2H), 6.76–6.90 (br s, 1H), 7.28–7.40 (m, 5H), 7.47–7.51 (m, 2H), 7.78–7.82 (m, 2H), 8.02 (s, 1H), 9.10 (s, 1H).

5.2.12. Compound 5c

White solid (99% yield), mp >230 °C. ^{1}H NMR (DMSO-d_6): δ 4.33 (d, J = 5.61 Hz, 2H), 5.56 (s, 2H), 6.80 (t, J = 5.65 Hz, 1H), 7.16–7.24 (m, 2H), 7.35–7.42 (m, 2H), 7.46–7.50 (m, 2H), 7.78–7.82 (m, 2H), 8.03 (s, 1H), 9.03 (s, 1H), 12.25–12.84 (br s, 1H).

5.2.13. Compound 6a

Off white solid (82% yield), mp 185–189 °C. ^{1}H NMR (DMSO-d_6): δ 4.29 (d, J = 5.56 Hz, 2H), 5.92 (s, 2H), 6.74 (t, J = 5.72 Hz, 1H), 7.24–7.49 (m, 7H), 7.57–7.61 (m,1H), 7.91 (s, 1H), 8.06 (t, J = 1.78 Hz, 1H), 8.96 (s, 1H), 12.78–13.15 (br s, 1H).

5.2.14. Compound 6b

Light green powder (88% yield), mp 192–194 °C. ^{1}H NMR (DMSO-d_6): δ 4.33 (d, J = 5.60 Hz, 2H), 5.57 (s, 2H), 6.65 (t, J = 5.63 Hz, 1H), 7.25–7.39 (m, 6H), 7.45–7.49 (m, 1H), 7.55–7.60 (m, 1H), 8.02 (s, 1H), 8.04–8.06 (m,1H), 8.80 (s, 1H), 12.64–13.06 (br s, 1H).

5.2.15. Compound 7a

To a solution of acid **5a** (0.5 g; 1.30 mmol) in anhydrous THF (20 mL) was added CDI (0.21 g; 1.304 mmol) and the mixture was refluxed for 20 min. 4-Phenoxyaniline (0.24 g; 1.30 mmol) was added and the mixture was stirred at room temperature for 2 h. The precipitate formed was collected by suction filtration to give **7a** as an off-white solid (0.23 g; 33% yield). ^{1}H NMR (DMSO-d_6): δ 4.32 (d, J = 5.60 Hz, 2H), 5.93 (s, 2H), 6.81 (t, J = 5.67 Hz, 1H), 6.96–7.14 (m, 5H), 7.23–7.43 (m, 8H), 7.50–7.57 (m, 2H), 7.74–7.81 (m, 2H), 7.93 (s, 2H), 9.01 (s, 1H), 10.09 (s, 1H). HRMS (ESI): Calcd for $C_{30}H_{26}N_6O_3SNa$ (M+Na) 573.1685; Found 573.1689.

5.2.16. Compound 7b

White solid (89% yield), mp 182–183 °C. ^{1}H NMR (DMSO-d_6): δ 4.30 (d, J = 5.63 Hz, 2H), 4.45 (d, J = 5.99 Hz, 2H), 5.93 (s, 2H), 6.90 (t, J = 5.40 Hz 1H), 7.20–7.49 (m,12H), 7.79 (d, J = 8.83 Hz, 2H), 7.92 (s, 1H), 8.86 (d, J = 5.98 Hz, 1H), 9.04 (s, 1H). HRMS (ESI): Calcd for $C_{25}H_{24}N_6O_2SNa$ (M+Na) 495.1579; Found 495.1596.

5.2.17. Compound 7c

White solid (68% yield), mp 201–202 °C. ^{1}H NMR (DMSO-d_6): δ 2.82 (t, J = 7.45 Hz, 2H), 3.41–3.49 (m, 2H), 4.30 (d, J = 5.59 Hz, 2H), 5.92 (s, 2H), 6.83 (t, 5.64 Hz, 1H), 7.19–7.35 (m, 8H), 7.38–7.46 (m, 4H), 7.70–7.73 (m, 2H), 7.91 (s, 1H), 8.36 (t, J = 5.64 Hz, 1H), 8.96 (s, 1H). HRMS (ESI): Calcd for $C_{26}H_{26}N_6O_2SNa$ (M+Na) 509.1736; Found 509.1730.

5.2.18. Compound 7d

Off white solid (88% yield), mp 190–191 °C. ^{1}H NMR (DMSO-d_6): δ 4.29–4.35 (m, 2H), 5.94 (s, 2H), 6.76 (t, J = 5.71 Hz, 1H), 7.04–7.10 (m, 2H), 7.24–7.36 (m, 5H), 7.39–7.43 (m, 2H), 7.48–7.55 (m, 2H), 7.74–7.93 (m, 4H), 8.98 (s, 1H), 10.05 (s, 1H). HRMS (ESI): Calcd for $C_{24}H_{22}N_6O_2SNa$ (M+Na) 481.1423; Found 481.1439.

Table 3
Inhibition of DENV2 and WNV NS2B/NS3pro protease by compounds **7g**, **7n**, **7t** and **8c**

Inhibitors	DENV2		WNV	
	% Inhibition at 10 μM	% Inhibition at 25 μM	% Inhibition at 10 μM	% Inhibition at 25 μM
7g	39.41 ± 2.69	52.54 ± 3.21	46.51 ± 1.75	57.95 ± 0.71
7n	55.31 ± 1.39	76.01 ± 0.96	58.78 ± 1.62	82.26 ± 1.04
7t	41.06 ± 1.83	56.98 ± 1.81	44.45 ± 2.08	60.85 ± 2.46
8c	40.27 ± 1.11	58.21 ± 4.31	49.28 ± 1.87	60.27 ± 2.36

WNV protease = 28 nM; DENV2 protease = 25 nM.

Table 4
Kinetics parameters for the tetra-peptide substrate and compound **7n** against WNV NS2B/NS3pro at 37 °C

7n (μM)	K_m (μM)	k_{cat} (s^{-1})	k_{cat}/K_m (M^{-1} s^{-1})
0	24.01 ± 0.62	0.060 ± 0.0013	2499 ± 99
1	26.04 ± 0.75	0.059 ± 0.0014	2274 ± 100
3	34.16 ± 1.88	0.062 ± 0.0018	1811 ± 163
5	36.90 ± 2.36	0.055 ± 0.0020	1503 ± 162

5.2.19. Compound 7e

Light brown solid (90% yield), mp 146–148 °C. ^{1}H NMR (DMSO-d_6): δ 4.31 (d, *J* = 5.55 Hz, 2H), 4.44 (d, *J* = 5.62 Hz, 2H), 5.93 (s, 1H), 6.86 (t, *J* = 5.50 Hz, 1H), 7.04 (br s, 2H), 7.22–7.92 (m, 11H), 8.79 (t, *J* = 5.71 Hz, 1H), 9.02 (s, 1H). HRMS (ESI): Calcd for $C_{23}H_{22}N_6O_3SNa$ (M+Na) 485.1372; Found 485.1373.

5.2.20. Compound 7f

Off white solid (46% yield), mp 184–185 °C. ^{1}H NMR (DMSO-d_6): δ 2.40–2.45 (m, 8H), 3.56 (t, *J* = 4.45 Hz, 4H), 4.30 (d, *J* = 5.57 Hz, 2H), 5.93 (s, 2H), 6.89 (t, *J* = 5.18 Hz, 1H), 7.24–7.47 (m, 7H), 7.71–7.73 (m, 2H), 7.92 (s, 1H), 8.21 (t, *J* = 5.80 Hz, 1H), 9.02 (s, 1H). HRMS (ESI): Calcd for $C_{24}H_{30}N_3O_7S$ (M+H) 496.2131; Found 496.2114.

5.2.21. Compound 7g

Light pink solid (47% yield), mp >230 °C. ^{1}H NMR (DMSO-d_6): δ 4.35 (d, *J* = 5.56 Hz, 2H), 5.58 (s, 2H), 6.77 (t, *J* = 5.67 Hz, 1H), 6.96–7.05 (m, 4H), 7.08–7.14 (m, 1H), 7.31–7.41 (m, 7H), 7.53 (d, *J* = 8.78 Hz, 2H), 7.75–7.80 (m, 2H), 7.87 (d, *J* = 8.77 Hz, 2H), 8.03(s, 1H), 8.95 (s, 1H), 10.08 (s, 1H). ^{13}C NMR (DMSO-d_6): δ 164.71, 157.27, 154.63, 151.71, 145.55, 143.43, 136.04, 135.17, 129.85, 128.62, 128.00, 127.85, 126.88, 122.84, 122.70, 122.57, 121.88, 119.18, 117.75, 116.53, 52.61, 34.74. HRMS (ESI): Calcd for $C_{30}H_{26}N_6O_3SNa$ (M+Na) 541.1964; Found 541.1956.

5.2.22. Compound 7h

White solid (54% yield), mp 213–214 °C. ^{1}H NMR (DMSO-d_6): δ 4.33 (d, *J* = 5.56 Hz, 2H), 4.45 (d, *J* = 5.96 Hz, 2H), 5.57 (s, 2H), 6.74 (t, *J* = 5.53 Hz, 1H), 7.30–7.40 (m, 10H), 7.44–7.48 (m, 2H), 7.76–7.82 (m, 2H), 8.02 (s, 1H), 8.78–8.94 (m, 2H). HRMS (ESI): Calcd for $C_{25}H_{24}N_6O_2SNa$ (M+Na) 463.1858; Found 463.1844.

5.2.23. Compound 7i

White solid (62% yield), mp 230 °C. 1H NMR (DMSO-d_6): δ 2.82 (t, *J* = 7.0 Hz, 2H), 3.41–3.48 (m, 2H), 4.33 (d, *J* = 5.57 Hz, 2H), 5.57 (s, 2H), 6.74 (t, *J* = 5.59 Hz, 1H), 7.16–7.40 (m, 10H), 7.42–7.47 (m, 2H), 7.70–7.73 (m, 2H), 8.02 (s, 1H), 8.38 (t, *J* = 5.65 Hz,1H), 8.87 (s, 1H). HRMS (ESI): Calculated for $C_{26}H_{26}N_6O_2SNa$ (M+Na) 477.2015; found 477.2036.

5.2.24. Compound 7j

White solid (35% yield), mp >230 °C. ^{1}H NMR (DMSO-d_6): δ 4.35 (d, *J* = 5.56 Hz, 2H), 5.58 (s, 2H), 6.75 (t, *J* = 5.56 Hz, 1H), 7.07 (t,

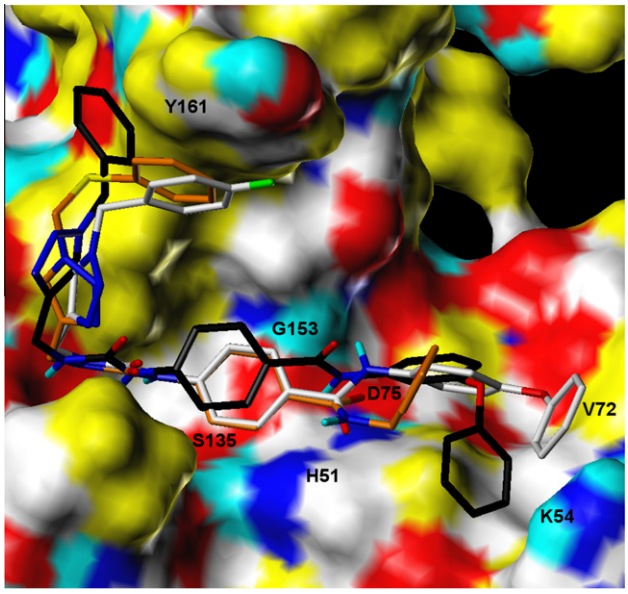

Figure 5A. Computationally predicted conformation of compounds **7a**, **7n** and **8f** bound to the catalytic site of DENV2 NS2B/NS3 protease. Ligands are rendered as CPK-colored sticks with the exception of carbon atoms (**7a**: orange, **7n**: white, **8f**: black), while the receptor surface is colored as follows: yellow = hydrophobic, white = polarized alkyl or aryl groups, cyan = polar hydrogens, blue = polar nitrogens and red = polar oxygens.

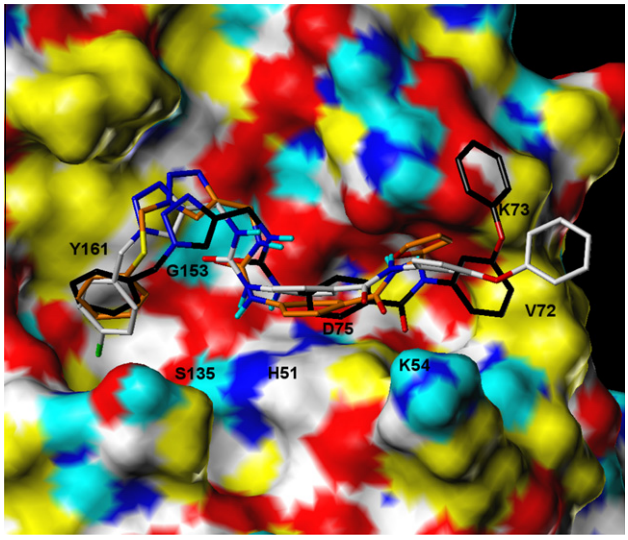

Figure 5B. Computationally predicted conformation of compound **7n** bound to the catalytic site of WNV NS2B/NS3 protease. Ligands are rendered as CPK-colored sticks with the exception of carbon atoms (**7a**: orange, **7n**: white, **8f**: black), while the receptor surface is colored as follows: yellow = hydrophobic, white = polarized alkyl or aryl groups, cyan = polar hydrogens, blue = polar nitrogens and red = polar oxygens.

J = 7.37 Hz, 1H), 7.29–7.40 (m, 7H), 7.50–7.54 (m, 2H), 7.74–7.78 (m, 2H), 7.85–7.90 (m, 2H), 8.03 (s, 1H), 8.94 (s, 1H), 10.04 (s, 1H). HRMS (ESI): Calculated for $C_{24}H_{22}N_6O_2SNa$ (M+Na) 449.1702; found 449.1722.

5.2.25. Compound 7k

White solid (35% yield), mp 207–208 °C. ^{1}H NMR (DMSO-d_6): δ 4.33 (d, *J* = 5.56 Hz, 2H), 4.43 (d, *J* = 5.66 Hz, 2H), 5.57 (s, 2H), 6.24–6.25 (m, 1H), 6.38–6.39 (m, 1H), 6.76 (t, *J* = 5.59 Hz, 1H), 7.28–7.40 (m, 5H), 7.42–7.46 (m, 2H), 7.56–7.57 (m, 1H), 7.74–7.78 (m, 2H), 8.02 (s, 1H), 8.76(t, *J* = 5.80 Hz, 1H), 8.89 (s, 1H). HRMS (ESI): Calcd for $C_{23}H_{22}N_6O_3SNa$ (M+Na) 453.1651; Found 453.1651.

5.2.26. Compound 7l

White solid (45% yield), mp 204–206 °C. ^{1}H NMR (DMSO-d_6): δ 2.36–2.45 (m, 6H), 3.33–3.37 (m, 2H), 3.56 (t, *J* = 4.59 Hz, 4H), 4.33 (d, *J* = 5.57 Hz, 2H), 5.57 (s, 2H), 6.77 (t, *J* = 5.63 Hz, 1H), 7.29–7.39 (m, 5H), 7.42–7.45 (m, 2 H), 7.70–7.73 (m, 2H), 8.02 (s, 1H), 8.21 (t, *J* = 5.67 Hz, 1H), 8.91(s, 1H). HRMS (ESI): Calcd for $C_{24}H_{30}N_7O_3$ (M+H) 464.2410; Found 464.2422.

5.2.27. Compound 7m

Light pink solid (25% yield), mp 199–200 °C. ^{1}H NMR (DMSO-d_6): δ 4.34 (d, *J* = 5.55 Hz, 2H), 5.57 (s, 2H), 6.72–6.77 (m, 2H), 7.02–7.07 (m, 2H), 7.12–7.18 (m, 1H), 7.30–7.44 (m, 8H), 7.49–7.58 (m, 4H), 7.82–7.85 (m, 2H), 8.02 (s, 1H), 8.94 (s, 1H), 10.10 (s, 1H). HRMS (ESI): Calcd for $C_{30}H_{26}N_6O_3Na$ (M+Na) 541.1964; Found 541.1932.

5.2.28. Compound 7n

White solid (49% yield), mp >230 °C. ^{1}H NMR (DMSO-d_6): δ 4.32 (d, *J* = 5.59 Hz, 2H), 5.55 (s, 2H), 6.71 (t, *J* = 5.62 Hz, 1H), 6.93–7.04 (m, 4H), 7.05–7.12 (m, 1H), 7.14–7.24 (m, 2H), 7.32–7.42 (m, 4H), 7.47–7.52 (m, 2H), 7.72–7.80 (m, 2H), 7.82–7.90 (m, 2H), 8.02 (s, 1H), 8.91 (s, 1H), 10.06 (s, 1H). ^{13}C NMR (DMSO-d_6): δ 164.72, 162.97, 160.54, 157.28, 154.64, 151.73, 145.62, 143.44, 135.18, 132.34, 130.24, 129.87, 128.54, 126.90, 122.86, 122.59, 121.85, 119.17, 117.77, 116.51, 115.58, 115.37, 51.80, 34.74. HRMS (ESI): Calcd for $C_{30}H_{25}FN_6O_3Na$ (M+Na) 559.1870; Found 559.1859.

5.2.29. Compound 7o

White solid (91% yield), mp 208–209 °C. ^{1}H NMR (DMSO-d_6): δ 4.33 (d, *J* = 5.56 Hz, 2H), 4.45 (d, *J* = 5.94 Hz, 2H), 5.56 (s, 2H), 6.98 (t, *J* = 5.58 Hz, 1H), 7.15–7.26 (m, 3H), 7.28–7.33 (m, 4H), 7.34–7.43 (m, 2H), 7.46–7.49 (m, 2H), 7.77–7.80 (m, 2H), 8.03 (s, 1H), 8.85 (t, *J* = 5.95 Hz, 1H), 9.10 (s, 1H). HRMS (ESI): Calcd for $C_{25}H_{23}FN_6O_2Na$ (M+Na) 481.1761; Found 481.1754.

5.2.30. Compound 7p

White solid (90% yield), mp 207–209 °C. ^{1}H NMR (DMSO-d_6): δ 2.82 (t, *J* = 7.46 Hz, 2H), 3.43 (m, 2H), 4.33 (d, *J* = 5.55 Hz, 2H), 5.56 (s, 2H), 7.05 (t, *J* = 5.56 Hz, 1H), 7.16–7.41 (m, 9H), 7.46 (d, *J* = 8.79 Hz, 2H), 7.71 (d, *J* = 8.75 Hz, 2H), 8.03 (s, 1H), 8.38 (t, *J* = 5.55 Hz, 1H), 9.17 (s, 1H). HRMS (ESI): Calcd for $C_{26}H_{25}FN_6O_2Na$ (M+Na) 495.1921; Found 495.1921.

5.2.31. Compound 7q

White solid (46% yield), mp >230 °C. ^{1}H NMR (DMSO-d_6): δ 4.35 (d, *J* = 5.55 Hz, 2H), 5.57 (s, 2H), 6.86 (t, *J* = 5.62 Hz, 1H), 7.04–7.09 (m, 1H), 7.17–7.43 (m, 7H), 7.53 (d, *J* = 8.78 Hz, 1H), 7.75–7.79 (m, 2H), 7.88 (d, *J* = 8.75 Hz, 2H), 8.04 (s, 1H), 9.12 (s, 1H), s (10.06, 1H). HRMS (ESI): Calcd for $C_{24}H_{21}FN_6O_2Na$ (M+Na) 467.1608; Found 467.1594.

5.2.32. Compound 7r

White solid (99% yield), mp 189–191 °C. ^{1}H NMR (DMSO-d_6): δ 4.33 (d, *J* = 5.60 Hz, 2H), 4.43 (d, *J* = 5.65 Hz, 2H), 5.56 (s, 2H), 6.24–6.25 (m, 1H), 6.37–6.39 (m, 1H), 6.79–6.86 (m, 1H), 7.02 (s, 1H), 7.16–7.24 (m, 2H), 7.34–7.50 (m, 4H), 7.72–7.83 (m, 2H), 8.03 (s, 1H), 8.76 (t, *J* = 5.70 Hz, 1H), 9.00 (s, 1H). HRMS (ESI): Calcd for $C_{23}H_{21}FN_6O_3Na$ (M+Na) 471.1557; Found 471.1555.

5.2.33. Compound 7s

(90% Yield), mp 163–166 °C. ^{1}H NMR (DMSO-d_6) δ 2.35–2.47 (m, 8H), 3.51- 3.63 (m, 4H), 4.32 (d, *J* = 5.56 Hz, 2H), 5.56 (s, 2H), 6.83 (t, *J* = 5.62 Hz, 1H), 7.01 (s, 1H), 7.16–7.24 (m, 2H), 7.36–7.47 (m, 4H), 7.69–7.73 (m, 2H), 8.02 (s, 1H), 8.21 (t, *J* = 5.64 Hz, 1H), 9.01 (s, 1H). HRMS (ESI): Calcd for $C_{24}H_{29}FN_7O_3$ (M+Na) 482.2316; Found 482.2297.

5.2.34. Compound 7t

Off white solid (16% yield), mp 211–212 °C. ^{1}H NMR (DMSO-d_6): δ 4.34 (d, *J* = 5.50 Hz, 2H), 5.56 (s, 2H), 6.69–6.80 (m, 2H), 7.00–7.09 (m, 2H), 7.10–7.27 (m, 3H), 7.29–7.46 (m, 5H), 7.47–7.62 (m, 4H), 7.84 (d, *J* = 8.78 Hz, 2H), 8.03 (s, 1H), 8.95 (s, 1H), 10.10 (s, 1H). ^{13}C NMR (DMSO-d_6): δ 164.96, 162.97, 160.54, 156.75, 156.43, 154.61, 145.61, 143.56, 140.89, 132.34, 130.24, 129.95, 128.66, 126.71, 123.39, 122.63, 118.68, 116.46, 115.58, 115.37, 114.89, 109.95, 51.79, 34.74. HRMS (ESI): Calcd for $C_{30}H_{25}FN_6O_3Na$ (M+Na) 559.1870; Found 559.1862.

5.2.35. Compound 8a

White solid (21% yield), mp 156–157 °C. ^{1}H NMR (DMSO-d_6): δ 4.30 (d, *J* = 5.64 Hz, 2H), 4.45 (d, *J* = 5.99 Hz, 2H), 5.93 (s, 2H), 6.65 (t, *J* = 5.67 Hz, 1H), 7.22–7.44 (m, 12H), 7.56–7.61(m, 1H), 7.85 (t, *J* =1.79 Hz, 1H), 7.91 (s, 1H), 8.75 (s, 1H), 8.97 (t, *J* = 6.07 Hz, 1H). HRMS (ESI): Calcd for $C_{25}H_{24}N_6O_2SNa$ (M+Na) 495.1579; Found 495.1567.

5.2.36. Compound 8b

White solid (57% yield), mp 155–156 °C. ^{1}H NMR (DMSO-d_6): δ 2.83 (t, *J* = 7.46 Hz, 2H), 3.45 (q, *J* = 6.30 Hz, 2H), 4.30 (s, 2H), 5.93 (s, 2H), 6.72 (br s, 1H), 7.19–7.42 (m, 12H), 7.55–7.59 (m, 1H), 7.79 (t, *J* = 1.80 Hz, 1H), 7.91 (s, 1H), 8.50 (t, *J* = 5.55 Hz, 1H), 8.83 (s, 1H). HRMS (ESI): Calcd for $C_{26}H_{26}N_6O_2SNa$ (M+Na) 509.1736; Found 509.1757.

5.2.37. Compound 8c

White solid (21% yield), mp 179–181 °C. ^{1}H NMR (DMSO-d_6): δ 4.30 (d, *J* = 5.65 Hz, 2H), 5.93 (s, 2H), 6.72–6.82 (m, 2H), 7.02–7.08 (m, 2H), 7.12–7.20 (m, 1H), 7.22–7.47 (m, 10H), 7.50–7.65 (m, 3H), 7.87 (t, *J* = 1.76 Hz, 1H), 7.91 (s, 1H), 8.90 (s, 1H), 10.28 (s, 1H). ^{13}C NMR (DMSO-d_6): δ 165.79, 156.79, 156.37, 154.89, 145.89, 140.70, 140.42, 135.42, 132.50, 130.25, 129.95, 129.84, 129.14, 128.54, 127.47, 123.43, 122.37, 120.63, 120.09, 118.71, 116.98, 114.87, 113.52, 109.93, 51.36, 34.69. HRMS (ESI): Calcd for $C_{30}H_{26}N_6O_3SNa$ (M+Na) 573.1685; Found 573.1693.

5.2.38. Compound 8d

White solid (80% yield), mp 162–164 °C. ^{1}H NMR (DMSO-d_6): δ 4.33 (d, *J* = 5.58 Hz, 2H), 4.45 (d, *J* = 5.97 Hz, 2H), 5.57 (s, 2H), 6.67 (t, *J* = 5.61 Hz, 1H), 7.2–7.42 (m, 12H), 7.57–7.60 (m, 1H), 7.84 (t, *J* = 1.64 Hz, 1H), 8.01 (s, 1H), 8.75 (s, 1H), 8.96 (t, *J* = 5.96 Hz, 1H). HRMS (ESI): Calcd for $C_{25}H_{24}N_6O_2Na$ (M+Na) 509.1736; Found 509.1757.

5.2.39. Compound 8e

White solid (83% yield), mp 197–198 °C. ^{1}H NMR (DMSO-d_6): δ 2.83 (t, *J* = 7.45 Hz, 2H), 3.41–3.49 (m, 2H), 4.33 (d, *J* = 5.56 Hz, 2H), 5.57 (s, 2H), 6.68 (t, *J* = 5.65 Hz, 1H), 7.17–7.40 (m, 12H), 7.55–7.58 (m, 1H), 7.78 (t, *J* = 1.65 Hz, 1H), 8.01 (s, 1H), 8.48 (t, *J* = 5.60 Hz,

1H), 8.74 (s, 1H). HRMS (ESI): Calcd for $C_{26}H_{26}N_6O_2Na$ (M+Na) 477.2015; Found 477.2032.

5.2.40. Compound 8f

White solid (64% yield), mp 201–202 °C. ^{1}H NMR (DMSO-d_6): δ 4.33 (d, J = 5.53 Hz, 2H), 5.57 (s, 2H), 6.69–6.79 (m, 2H),7.02–7.08 (m, 2H), 7.13–7.19 (m, 1H), 7.29–7.46 (m, 10H), 7.51–7.64 (m, 3H), 7.86 (s, 1H), 8.01 (s, 1H), 8.83 (s, 1H), 10.28 (s, 1H). HRMS (ESI): Calcd for $C_{30}H_{26}N_6O_3Na$ (M+Na) 541.1945; Found 541.1945.

6. Biochemistry

6.1. DENV2 NS2B/NS3pro expression and purification

The construction of the pQE30-NS2BH(QR)NS3pro expression plasmid has been described previously.[26] The protease was expressed from *Escherichia coli* strain Top 10 F' (Invitrogen) transformed by pQE30-NS2BH(QR)–NS3pro plasmid and purified as described.[28] DENV2 NS2B/NS3pro contains the hydrophilic NS2B cofactor peptide (NS2BH) linked to the N-terminal NS3 protease domain via Q-R (P2 and P1 residues at the NS2B–NS3 junction site).

6.2. WNV NS2B/NS3pro expression and purification

The expression and purification of the WNV NS2BH–NS3pro containing the five amino acid spacer between the NS2B and NS3pro domains was previously described.[28]

6.3. In vitro DENV2 and WNV NS2B/NS3pro assays and inhibition studies

The compounds were dissolved in dimethyl sulfoxide (DMSO) to make 50 mM stock solutions. The compounds were screened at 25 μM in 1% v/v DMSO in the final reaction mixture. Protease assays were performed in triplicates in Greiner Black 96 well plates. Each assay consisted of the reaction mixture of 100 μL containing 200 mM Tris–HCl buffer, pH 9.5, 30% glycerol, 25 nM DENV2 NS2B–NS3 pro (or 28 nM WNV NS2B/NS3pro) and the compound. The enzyme and the compound were pre-incubated at room temperature for 15 min prior to addition of the substrate (5 μM), Bz-Nle-Lys-Arg-Arg-AMC. The time course of the reaction at 37 °C was followed at every 90 s intervals for up to 30 min in a monochrometer-based spectrofluorometer (Molecular Devices, Sunnyvale, CA) at excitation and emission wavelengths of 380 and 460 nm, respectively. The percent inhibition for each compound at 25 μM was first determined. For determining IC_{50} values, twelve data points obtained from the range of 10, 50 nM, 0.1, 0.5, 1, 2, 4, 6, 8, 10, 20, and 25 μM inhibitor concentrations of selected compounds were used. IC_{50} values were calculated using the SigmaPlot 2001 v7.0 software.[40]

7. Kinetics analysis

To determine the K_m and V_{max} values of compound **7n**, four different concentrations of inhibitor (0, 1.0, 3.0 and 5.0 μM) were assayed at varying concentrations (0–50 μM) of substrate. The kinetics analysis methods have been previously described.[41] K_i values were calculated from these data using a secondary plot of $K_{m,app}$ against the concentrations of selected compound **7n** using SigmaPlot 2001 v7.0 software.[40]

8. Molecular modeling

Molecular docking simulations were performed with the Surflex program.[42] The DENV NS3/NS2B receptor was modeled from the active form crystal structure of Noble et al. (PDB ID: 3U1I)[12] by extracting all ligands and waters, and protonating the receptor according to assumption of anionic aspartate and glutamate groups, and cationic arginines and lysines). The WNV NS2B/NS3pro receptor model was prepared in an analogous manner using the crystal structure of Erbel et al. (PDB ID 2FP7).[13] In both cases, the co-crystallized ligand was used to define the Surflex protomol structure (which guides the original ligand binding site prediction), and five distinct randomized starting conformations and 100 final conformations were specified for the ligand. Ligands were constructed and refined according to default molecular mechanics constraints, force fields and optimization settings via the SYBYL 8.1 program (Tripos Associates, St. Louis, MO, 2009).

Acknowledgments

The generous financial support of this work by the National Institutes of Health (AI082068) is gratefully acknowledged.

References and notes

1. Lindenbach, B. D.; Thiel, H.-J.; Rice, C. M., 5th ed. In *Fields Virology*; Knipe, D. M., Howley, P. M., Eds.; Lippincott, Williams and Wilkins: Philadelphia, 2007; Vol. 1, pp 1101–1152.
2. Stevens, A. J.; Gahan, M. E.; Mahalingam, S.; Keller, P. A. *J. Med. Chem.* **2009**, *52*, 7911.
3. Cregar-Hernandez, L.; Jiao, G.-S.; Johnson, A. T.; Lehrer, A. T.; Wong, T. A. S.; Margosiak, S. A. *Antiviral Chem. Chemother.* **2011**, *21*, 209.
4. Noble, C. G.; Chen, Y.-L.; Dong, H.; Gu, F.; Lim, S. P.; Schull, W.; Wang, Q.-Y.; Shi, P.-Y. *Antiviral Res.* **2010**, *85*, 450.
5. Sampath, A.; Padmanabhan, R. *Antiviral Res.* **2009**, *81*, 6.
6. Lescar, J.; Luo, D.; Xu, T.; Sampath, A.; Lim, S. P.; Canard, B.; Vasudevan, S. G. *Antiviral Res.* **2008**, *80*, 94.
7. Yusof, R.; Clum, S.; Wetzel, M.; Murthy, H. M.; Padmanabhan, R. *J. Biol. Chem.* **2000**, *275*, 9963.
8. Natarajan, S. *Genet. Mol. Biol.* **2010**, *33*, 214.
9. Schechter, I.; Berger, A. *Biochem. Biophys. Res. Commun.* **1967**, *27*, 157.
10. Niyomrattanakit, P.; Winoyanuwattikun, P.; Chanprapaph, S.; Angsuthanasombat, C.; Panyim, S.; Katzenmeier, G. *J. Virol.* **2004**, *78*, 13708.
11. Wichapong, K.; Pianwanit, S.; Sippl, W.; Kokpol, S. *J. Mol. Recognit.* **2010**, *23*, 283.
12. Noble, C. G.; She, C. C.; Chao, A. T.; Shi, P. Y. *J. Virol.* **2012**, *86*, 438.
13. Erbel, P.; Schiering, N.; D'Arcy, A.; Renatus, M.; Kroemer, M.; Lim, S. P.; Yin, Z.; Keller, T. H. *Nat. Struct. Mol. Biol.* **2006**, *13*, 372.
14. de la Cruz, L.; Nguyen, T. H.; Ozawa, K.; Shin, J.; Graham, B.; Huber, T.; Otting, G. *J. Am. Chem. Soc.* **2011**, *133*, 19205.
15. Schuller, A.; Yin, Z.; Chia, B. C. S.; Doan, D. N. P.; Kim, H.-K.; Shang, L.; Loh, T. P.; Hill, J.; Vasudevan, S. G. *Antiviral Res.* **2011**, *92*, 96.
16. Yin, Z.; Patel, S. J.; Wang, W. L.; Wang, G.; Chan, W. L.; Rao, K. R.; Alam, J.; Jeyaraj, D. A.; Ngew, X.; Patel, V.; Beer, D.; Lim, S. P.; Vasudevan, S. G.; Keller, T. H. *Bioorg. Med. Chem. Lett.* **2006**, *16*, 36.
17. Yin, Z.; Patel, S. J.; Wang, W. L.; Chan, W. L.; RangaRao, K. R.; Ngew, X.; Patel, V.; Beer, D.; Knox, J. E.; Ma, N. L.; Ehrhardt, C.; Lim, S. P.; Vasudevan, S. G.; Keller, T. H. *Bioorg. Med. Chem. Lett.* **2006**, *16*, 40.
18. Knox, J. E.; Ma, N. L.; Yin, Z.; Patel, S. J.; Wang, W. L.; Wang, G.; Chan, W. L.; Vanga Rao, K. R.; Wang, G.; Ngew, X.; Patel, V.; Beer, D.; Lim, S. P.; Vasudevan, S. G.; Keller, T. H. *J. Med. Chem.* **2006**, *49*, 6585.
19. Steuer, C.; Gege, C.; Fischl, W.; Heinonen, K. H.; Bartenschlager, R.; Klein, C. D. *Bioorg. Med. Chem.* **2011**, *19*, 4067.
20. Bodenreider, C.; Beer, D.; Keller, T. H.; Sonntag, S.; Wen, D.; Yap, L.; Yau, Y. H.; Sochat, S. G.; Huang, D.; Zhou, T.; Caflisch, A.; Su, X.-C.; Ozawa, K.; Otting, G.; Vasudevan, S. G.; Lescar, J.; Lim, S. P. *Anal. Biochem.* **2009**, *395*, 195.
21. Nitsche, C.; Steuer, C.; Klein, C. D. *Bioorg. Med. Chem.* **2011**, *19*, 7318.
22. Nitsche, C.; Behnam, M. A. M.; Steuer, C.; Klein, C. D. *Antiviral Res.* **2012**, *94*, 72.
23. Tiew, K. C.; Dou, D.; Teramoto, T.; Lai, H.; Alliston, K. R.; Lushington, G. H.; Padmanabhan, R.; Groutas, W. C. *Bioorg. Med. Chem.* **2012**, *20*, 1213.
24. Parkinson, T.; Pryde, D. C. *Future Med. Chem.* **2010**, *2*, 1181.
25. (a) Kolb, H. C.; Finn, M. G.; Sharpless, K. B. *Angew. Chem., Int. Ed.* **2004**, *2001*, 40; (b) Shen, J.; Woodward, R.; Kedenburg, J. P.; Liu, X.; Chen, M.; Fang, L.; Sun, D.; Wang, P. G. *J. Med. Chem.* **2008**, *51*, 7417.
26. Yon, C.; Teramoto, T.; Mueller, N.; Phelan, J.; Ganesh, V. K.; Murthy, K. H.; Padmanabhan, R. *J. Biol. Chem.* **2005**, *280*, 27412.
27. Yusof, R. S.; Clum, M.; Wetzel, H.; Murthy, H. M.; Padmanabhan, R. *J. Biol. Chem.* **2000**, *265*, 9963.
28. Mueller, N. H.; Yon, C.; Ganesh, V. K.; Padmanabhan, R. *Int. J. Biochem. Cell Biol.* **2007**, *39*, 606.
29. Dou, D.; Viwanathan, P.; Li, Y.; He, G.; Alliston, K. R.; Lushington, G. H.; Brown-Clay, J. D.; Padmanabhan, R.; Groutas, W. C. *J. Comb. Chem.* **2010**, *12*, 836.

30. Li, J.; Lim, P.; Beer, D.; Patel, V.; Wen, D.; Tumanut, C.; Tully, D. C.; Williams, J. A.; Jiricek, J.; Priestle, J. P.; Harris, J. L.; Vasudevan, S. G. *J. Biol. Chem.* **2005**, *280*, 28766.
31. Mueller, N. H.; Pattabiraman, N.; Ansarah-Sobrinho, C.; Viswanathan, P.; Pierson, T. C.; Padmanabhan, R. *Antimicrob. Agents Chemother.* **2008**, *52*, 3385.
32. Gleeson, M. *J. Med. Chem.* **2008**, *51*, 817.
33. Lipinski, C. A.; Lombardo, F.; Dominy, B. W.; Feeney, P. J. *Adv. Drug Delivery Rev.* **1997**, *23*, 3.
34. Keller, T. H.; Pichota, A.; Yin, Z. *Curr. Opin. Chem. Biol.* **2006**, *10*, 357.
35. Johnson, T. W.; Dress, K. R.; Edwards, M. *Bioorg. Med. Chem. Lett.* **2009**, *19*, 5560.
36. Perola, E. *J. Med. Chem.* **2010**, *53*, 2986.
37. Leeson, P. D.; Empfield, J. R. *Annu. Rep. Med. Chem.* **2010**, *45*, 393.
38. Walters, W. P.; Green, J.; Weiss, J. R.; Murcko, M. A. *J. Med. Chem.* **2011**, *54*, 6405.
39. Waring, M. J. *Expert Opin. Drug Discov.* **2010**, *5*, 235.
40. Systat Software Inc., San Jose, CA.
41. Ezgimen, M.; Lai, H.; Mueller, N. H.; Lee, K.; Cuny, G.; Ostrov, D. A.; Padmanabhan, R. *Antiviral Res.* **2012**, *94*, 18.
42. Jain, A. N. *J. Med. Chem.* **2003**, *46*, 499.